

Massive Compact Stars as Quark Stars

Hilário Rodrigues

Centro Federal de Educação Tecnológica do Rio de Janeiro

Av Maracanã 249, 20271-110, Rio de Janeiro, RJ, Brazil

`harg@cefet-rj.br`

Sérgio Barbosa Duarte

Centro Brasileiro de Pesquisas Físicas

Rua Dr. Xavier Sigaud 150, 22290-180, Rio de Janeiro, RJ, Brazil

`sbd@cbpf.br`

and

José Carlos T. de Oliveira

Departamento de Física, Universidade Federal de Roraima

Campus do Paricarana s/n, 69310-270, Boa Vista, RR, Brazil

`jcto@cbpf.br`

Received _____; accepted _____

Not to appear in Nonlearned J., 45.

ABSTRACT

High massive compact stars have been reported recently in the literature, providing strong constraints on the properties of the ultradense matter beyond the saturation nuclear density. In view of these results, the calculations of quark star or hybrid star equilibrium structure must be compatible with the provided observational data. But, since the used equations of state describing quark matter are in general too soft, in comparison with the equation of states used to describe the hadronic or nuclear matter, the calculated quark star models presented in the literature are in general not suitable to explain the stability of high compact massive objects.

In this work, we present the calculations of spherically symmetric quark star structure by using an equation of state which takes into account the superconducting Color-Flavor Locked (CFL) phase of the strange quark matter. In addition, some fundamental aspects of QCD (asymptotic freedom and confinement) are considered by means of a phenomenological description of the deconfined quark phase, the density-dependent quark mass model (Chakrabarty et al 1989; Chakrabarty 1991). The quark matter behavior introduced by these model stiffens the corresponding equation of state. We thus investigate the influence of these models on the mass-radius diagram of quark stars. We obtain massive quark stars due to the stiffness of the equation of state, when a reasonable parametrization of the color superconducting gap is used. Models of quark stars enveloped by a nucleonic crust composed of a nuclear lattice embedded in an electron gas, with nuclei close to neutron drip line, are also discussed.

Subject headings: equation of state: stars: neutron — X-rays: individual (EXO 0748-676, EXO 1745-248, 4U 1608-52)

1. Introduction

The study of the structure of compact stars requires the understanding of the equation of state describing the stellar matter under extreme conditions. It has been pointed out that most of the current equations of state describing quark matter are too soft and so unable to explain the existence of massive neutron stars (Cottam et al 2002; Özel 2006). Only stiff equations of state describing normal nuclear matter at high densities would be capable of explaining the stability of high compact star masses ($M \sim 2 M_\odot$). Thus, apparently these observational data tend to favor the existence of matter without deconfined quarks in the interior of neutron stars. Examples of massive compact stars are the isolated neutron star RX J1856.5-3754 (Trumper et al 2008), some low-mass X-ray binaries, e.g., 4U 1636-536 (Barret et al 2005), and the neutron star J0751+1807 ($2.1 \pm 0.2 M_\odot$) (Nice et al 2005).

More recently, two possible pairs of values of mass and radius have been attributed to neutron star EXO 1745-248, one of them centered around $M = 1.4 M_\odot$ with radius $R = 11 \text{ km}$, and the other one centered around $M = 1.7 M_\odot$ and with a smaller radius $R = 9 \text{ km}$ (Özel et al 2008). The neutron star in the low-mass X-ray binary 4U 1608-52 has a mass determined as $M \geq (1.84 \pm 0.009) M_\odot$ and radius $R \geq (9.83 \pm 1.24) \text{ km}$ (Güver et al 2010). Regarding the neutron star EXO 0748 – 676, the obtained lower limits on the mass and radius are: $M \geq 2.10 \pm 0.28 M_\odot$ and $R \geq 13.8 \pm 1.8 \text{ km}$ (Özel 2006), even though these results are still unclear (Cottam et al 2002).

It is believed that at high densities the strange quark matter is a more stable configuration than the ordinary nuclear matter (Bodmer 1971; Witten 1984) and hence it is claimed that neutron stars would be stellar objects entirely or partially composed of strange quark matter (Itoh 1970; Weber 2005), that is, a quark star or a hybrid star. However, some used equations of state describing quark matter are too soft to support quark stars with large masses and then, in this scenario, quark stars or hybrid stars seem to be incompatible

with the observed massive neutron stars mentioned above. In fact, calculations using soft equations of state for quark matter provide values of maximum masses for hybrid neutron stars around $1.6 M_\odot$, and lower values of maximum masses for strange quark stars.

Stiff equations of state of quark matter can be obtained when effects of strong interaction are taken into account (Alford et al 2007). Calculations of compact star models using quark matter equation of state, generated by modified MIT bag model (including perturbative corrections to QCD) or by the Nambu-Jona-Lasinio model, are in general capable of reproducing a maximum star mass around $2 M_\odot$, which is compatible with the observational data (Alford et al 2005; Rodrigues et al 2010).

A recent calculation for cold and dense QCD strange quark matter including corrections to order $O(\alpha_s^2)$ indicates that massive compact stars with mass $\gtrsim 2M_\odot$ up to maximal masses $\sim 2.75M_\odot$ would be interpreted as possible candidates for strange quark stars, *i.e.*, compact stars composed entirely of deconfined u , d and s quarks, and that compact stars with observed masses up to $\sim 2M_\odot$ would be identified with hybrid stars, neutron stars with a central core made up of deconfined quark matter (Kurkela 2010). Motivated by these recent investigations, in this work we study the color superconducting quark matter by using a phenomenological model, namely the density-dependent quark mass model (Chakrabarty et al 1989; Chakrabarty 1991), in order to describe the strange quark star structure. Assuming the CFL phase is the ground state of strange quark matter, we consider the effects of the CFL gap energy on the global strange quark star structure.

The density-dependent quark mass model provides stiff equations of state, and hence large quark star masses can be obtained with this type of equations of state, which are compatible with some of those observational data, if reasonable values for the equation of state parameters are used. Note that these results contrast with the mass-radius relationships predicted by equations of state constructed with descriptions of quark matter

based on a simple version of the MIT bag model, as discussed in Ref. (Oliveira et al 2008).

The study of the structure of the nucleonic crusts is also presented, and our results for quark star mass versus radius are compared with the data presented recently by Özel in references (Özel 2006), (Özel et al 2008) and (Güver et al 2010).

This work is organized as follows. In Section 2 we describe the equation of state of the cold color superconducting strange quark matter. In Section 3 we study the equation of state of the unpaired quark matter (UQM) and discuss the color superconducting to unpaired quark matter phases. In Section 4 we present and discuss our results obtained for bare quark stars structure and compare them to some values of mass and radii derived from observational data. In Section 5 we present some results for quark stars with nucleonic crusts. Conclusions and final remarks are presented in Section 6.

2. Description of the cold color superconducting quark matter

In the last few years the study of color superconducting phase in quark-gluon plasma (Alford et al 1998, 1999; Alford 2004) has been attracting a great interest in discussing the possible states of quark matter. At QCD perturbative regime the attractive quark interaction introduces instabilities in the Fermi surface, producing a gap in the quasiparticle energy spectrum. The color and flavor symmetries of three-flavor QCD are hence broken down, leading to the formation of pairs of quarks (this mechanism is analogous to the electron pairing in the ordinary electric superconducting phenomenon). The quark matter becomes a color superconductor, with equal number of quarks for the three flavors u , d and s in an electrically neutral phase called Color-Flavor Locked (CFL) (Alford et al 2008; Braun-Muzinger & Wambach 2009). The color superconducting gap is included in an additional energy term to the thermodynamic potential associated to a quasi-free quark

system as it is done elsewhere (see for example the review article (Schmitt 2010)).

In order to describe the Color-Flavor Locked phase composed of free quarks u , d and s at zero temperature we use the thermodynamic potential density given by (Rajagopal & Wilczek 2001a)

$$\Omega = \sum_f \frac{3}{\pi^2} \int_0^\nu k^2 (\sqrt{k^2 + m_f^2} - \mu) dk + \Omega_{CFL}, \quad (1)$$

where m_f stand for the constituent quark masses, with $f = \{u, d, s\}$. In this equation, the first term in the right-hand side gives the contribution of degenerate quarks to the thermodynamic potential density, and the second one is the first order contribution from the quasiparticle energy gap, which reads

$$\Omega_{CFL} = -\frac{3}{\pi^2} \Delta_{CFL}^2 \mu^2, \quad (2)$$

where the quark chemical potential and the common Fermi momentum ν , considering $m_u = m_d$, are given respectively by

$$\mu = \frac{\mu_u + \mu_d + \mu_s}{3}, \quad (3)$$

and

$$\nu = \left[\left(2\mu - \sqrt{\mu^2 + \frac{m_s^2 - m_u^2}{3}} \right)^2 - m_u^2 \right]^{1/2}. \quad (4)$$

The above common Fermi momentum of the quark system depends on the mass of the three light quark flavors, and it does minimize the thermodynamic potential given by Eq. (1) in respect to the parameter ν . Note that for $m_u = m_d = 0$, one recovers the expression

$$\nu = 2\mu - \sqrt{\mu^2 + \frac{m_s^2}{3}}, \quad (5)$$

derived e.g. by Rajagopal and Wilczek (Rajagopal & Wilczek 2001a), who have considered massless up and down quarks, and the nonzero current mass of the strange quark in the calculations.

In the *CFL* phase described here, the three flavors of quarks satisfy the following conditions: (i) they have equal Fermi momenta, which minimizes the free energy of the system (Rajagopal & Wilczek 2001a; Orsaria et al 2007); (ii) they have equal number densities n_f , as a consequence of the first condition, which means that $n_f = \rho_B$ and $\mu_f = \mu$, for $f = \{u, d, s\}$; (iii) the quark system has neutral electromagnetic charge in bulk, as a direct consequence of the previous condition.

In the density-dependent quark mass model (Chakrabarty et al 1989; Chakrabarty 1991) the masses of the three lightest quarks scale inversely with the baryon number density, namely:

$$m_u = m_d = \frac{C}{3\rho_B} \quad \text{and} \quad m_s = m_{s0} + \frac{C}{3\rho_B}, \quad (6)$$

where C is interpreted as the constant energy density in the zero quark density limit, and is analogous to the QCD vacuum energy density present in the MIT bag model, and

$$\rho_B = \frac{n_u + n_d + n_s}{3}, \quad (7)$$

is the baryon number density expressed in terms of the quark number densities n_u , n_d and n_s . The current mass of the strange quark, m_{s0} , enters as a parameter of the model. The dependence of the quark masses on the baryon density mimics the quark interaction at different values of density, incorporating the effect of quark interactions in the model. Throught this artifact, the density-dependent quark mass model recovers the asymptotic behavior of quark matter predicted by QCD at high densities, namely, the quark asymptotic freedom and the dynamical confinement of quarks for low density regime as natural limit situations. Consequently, in this model quarks are dynamically massive, and thus chiral symmetry of the QCD Lagrangian is dynamically broken. Besides, as mentioned previously, it would be unrealistic adopting vanishing dynamical quark masses to describe quark matter for the range of densities currently accepted for the interior of compact stars (Schmitt 2010).

The pressure derived from the thermodynamic potential in equation (1) thus reads

$$P = -\Omega + B^*. \quad (8)$$

The term B^* in the right-hand side of the last equation arises from the thermodynamic consistence between the degenerate quark gas pressure and the thermodynamic potential, due to the dependence of the quark mass on the baryon density. The additional term B^* is similar to QCD vacuum pressure present in the MIT bag model. The presence of this term enables a smooth model transition from the quark confinement regime to the asymptotic freedom since its explicitly form,

$$B^* = \rho_B \left. \frac{\partial \Omega}{\partial \rho_B} \right|_{T=0, \mu}, \quad (9)$$

is a decreasing function of the baryon density.

We thus found the following explicit expression for the pressure:

$$P = \sum_f \frac{3}{8\pi^2} m_f^4 \left[f(x) + \frac{4}{m_f} \frac{C}{3\rho_B} g(x) \right] + \frac{3}{\pi^2} (\nu^3 \mu + \Delta_{CFL}^2 \mu^2), \quad (10)$$

where the functions $f(x)$ and $g(x)$ are given by

$$f(x) = \ln [x + (x^2 + 1)^{1/2}] - x(x^2 + 1)^{1/2}(2x^2 + 1), \quad (11)$$

and

$$g(x) = \ln [x + (x^2 + 1)^{1/2}] - x(x^2 + 1)^{1/2}, \quad (12)$$

with x defined by

$$x = \frac{\nu}{m_f}. \quad (13)$$

Finally, the energy density can be obtained from the thermodynamic relation

$$\varepsilon = -P + \sum_f n_f \mu_f, \quad (14)$$

from which we find

$$\varepsilon_{CFL} = -P + 3\rho_B\mu. \quad (15)$$

In order to complete the description of the CFL quark matter phase, we write the quark number density,

$$n_f = - \left. \frac{\partial \Omega}{\partial \mu} \right|_{\rho_B}, \quad (16)$$

which gives the baryon number density

$$\rho_B = \frac{1}{\pi^2}(\nu^3 + 2\Delta_{CFL}^2\mu). \quad (17)$$

The condensation energy of the Cooper pairs in the CFL phase given by Eq. (2) (Alford et al 1999), requires the specification of the color superconducting gap. In order to make the present phenomenological approach compatible with microscopic treatments based on some results of QCD, here we use solutions provided by the Nambu-Jona-Lassinio (NJL) model with a local four-fermion interaction. A recent study in this direction discussing the solution of the gap equation is presented in Ref. (Rajagopal & Wilczek 2001b), where it is given the following approximate gap expression:

$$\Delta_{CFL} \simeq 2\sqrt{\Lambda^2 - \tilde{\mu}^2} \exp\left(\frac{\Lambda^2 - 3\tilde{\mu}^2}{2\tilde{\mu}^2}\right) \exp\left(-\frac{\pi^2}{8G_D\tilde{\mu}^2}\right), \quad (18)$$

where $G_D = \eta G_S$ is the strength of the diquark pairing, with G_S being the quark-antiquark coupling constant and η a dimensionless parameter between 3/4, for the intermediate coupling strength, and 1 corresponding to the strong coupling between quarks (Ruster et al 2005). In the above equation we have introduced a quark chemical potential shift, $\tilde{\mu} = \mu - \mu^*$, where μ^* establishes the quark chemical potential value for which the gap begins to take significant values.

At this point one can realize that the present calculation involves two parameters from the dynamical quark mass expression (C and m_{s0}) and the parameter μ^* to adjust the

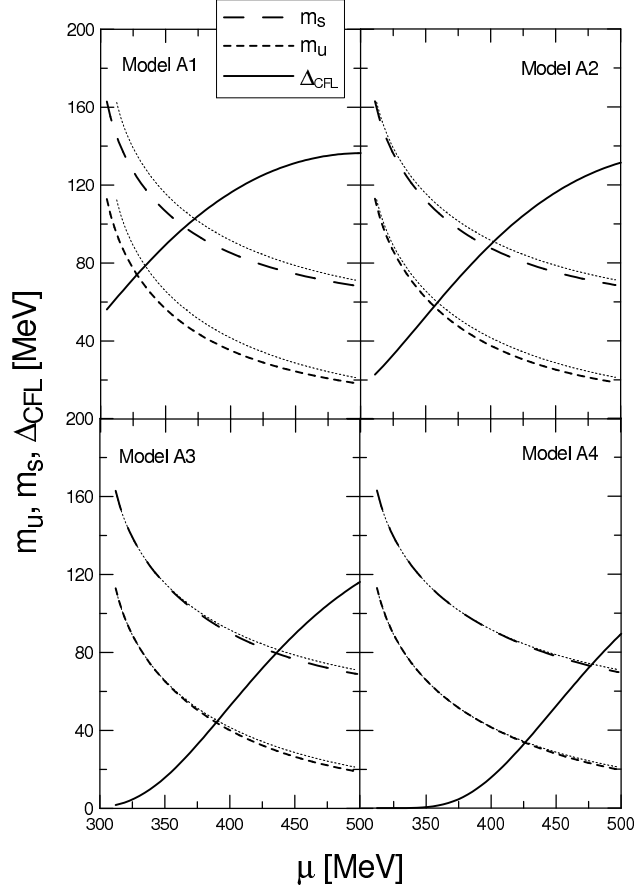


Fig. 1.— Dependence of the quark masses and the color superconducting gap on the quark chemical potential for the models A1, A2, A3, and A4 given in Table 1. The thin dotted curves near the constituent quark masses curves represent the corresponding constituent quark masses for the unpaired quark phase.

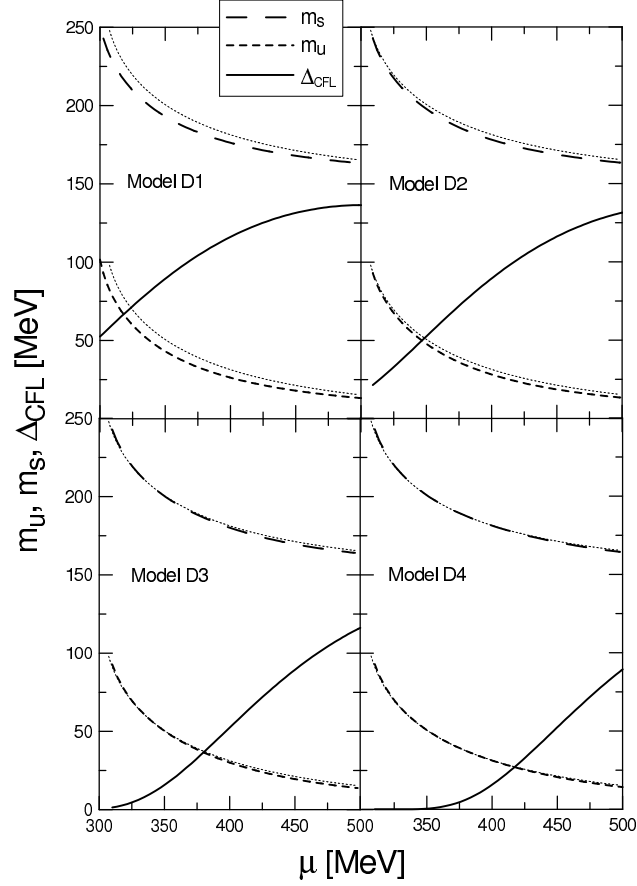


Fig. 2.— Dependence of the quark masses and the color superconducting gap on the quark chemical potential for the models D1, D2, D3, and D4 given in Table 1. The thin dotted curves near the constituent quark masses curves represent the corresponding constituent quark masses for the unpaired quark phase.

gap in the density region of interest. The values of the first pair of parameters are chosen according to the stability criterion applied to the strange quark matter energy per baryon, which reads $\epsilon/\rho_0 \leq 930 \text{ MeV}$ at normal nuclear density ρ_0 , where 930 MeV is the energy per baryon in iron nuclei (Oliveira et al 2008). The possible values of the parameter C lie in the interval $69.05 \leq C \leq 111.6 \text{ MeV} \cdot \text{fm}^{-3}$ and the strange quark mass lies in the interval $40 \leq m_{s0} \leq 180 \text{ MeV}$ (Lugones 1994). The current masses of up and down quarks are set $m_{u0} = m_{d0} = 0$. For the free parameter μ^* we have used the values 100, 150, 200, and 250 MeV to adjust the gap behavior properly in the range of densities covered by compact objects in analysis. Different combinations of the parameters values are considered in this work. In Table 1 we display the different sets of the model parameter values applied in the present study. For the whole calculation we have fixed $\Lambda = 603 \text{ MeV}$ and $G_S \Lambda^2 = 1.822$. We will consider only the case $G_D = G_S$ for the diquark coupling strength.

In figures 1 and 2 we show the dependence of the constituent quark masses and the color superconducting gap as functions of the quark chemical potential, for the cases A and D displayed in Table 1, covering four values of the free gap parameter μ^* . We can see that for $\mu^* = 100 \text{ MeV}$, the color superconducting phase dominates even for low values of the quark chemical potential. However, for higher values of the parameter μ^* , the unpaired phase dominates for low values of the quark chemical potential and thus we need to deal with a phase transition between the two phases. Similar behavior for the gap and the constituent masses is observed for the other sets of parameters given in Table 1. Consequently it is necessary to analyze phase transitions between the color superconducting and unpaired quark matter, as well as how sensitive is the phase transition to the parameter changes. We remark that the quark pairing lowers the constituent quark masses when compared to the values in the unpaired quark phase.

3. Color superconducting to unpaired quark matter phase transition

For the unpaired quark matter (UQM), the thermodynamic potential density reads

$$\Omega_{UQM} = \sum_f \frac{3}{\pi^2} \int_0^{\nu_f} k^2 (\sqrt{k^2 + m_f^2} - \mu_f) dk, \quad (19)$$

with $f = \{u, d, s\}$ and where ν_f is the Fermi momentum of each quark flavor, which is given by

$$\nu_f = \sqrt{\mu_f^2 - m_f^2}. \quad (20)$$

The number density of each quark flavor is defined by

$$n_f = - \left. \frac{\partial \Omega_{UQM}}{\partial \mu_f} \right|_{\rho_B}, \quad (21)$$

which provides explicitly

$$n_f = \frac{1}{\pi^2} (\mu_f^2 - m_f^2)^{3/2}. \quad (22)$$

For degenerate and massless free electrons, the free energy density is given by

$$\Omega_e = - \frac{1}{12\pi^2} \mu_e^4, \quad (23)$$

and thus the electron number density reads

$$n_e = \frac{1}{3\pi^2} \mu_e^3. \quad (24)$$

In beta equilibrium, the chemical potentials of quarks and electrons must satisfy the following relationships:

$$\mu_d = \mu_u + \mu_e, \quad \mu_s = \mu_d. \quad (25)$$

The condition of electric charge neutrality provides the equation

$$\frac{2}{3}n_u - \frac{1}{3}n_d - \frac{1}{3}n_s - n_e = 0. \quad (26)$$

Note that the existence of different quark masses turns impossible for the unpaired quark matter to satisfy equations (25) and (26) simultaneously, without the presence of electrons in bulk.

In order to analyze the occurrence of the phase transition, the behavior of the quark matter pressure as a function of the quark chemical potential is depicted in the Fig. 3 for all sets of parameters combination given in Table 1. For the class A models, we can identify subtle intersections of the pressure curves for the cases A3 and A4 with the curve of the unpaired phase, which indicate the phase transitions between the two phases, occurring at $\mu \simeq 335 \text{ MeV}$ (case A3) and at $\mu \simeq 390 \text{ MeV}$ (case A4). For the set of parameters D2, D3 and D4 the phase transition between the two phases occurs at $\mu \simeq 333 \text{ MeV}$ (case D2), $\mu \simeq 370 \text{ MeV}$ (case D3), and at $\mu \simeq 413 \text{ MeV}$ (case D4). For the last one, the phase transition occurs at a baryon density $\rho \simeq 5.5\rho_0$, with $\rho_0 = 0.15 \text{ fm}^{-3}$ being the normal nuclear matter density. We remark that small values of the parameter μ^* combined with the high values of the current strange quark mass provide stiffer equations of state, leading to more massive quark stars, as we will discuss latter.

4. Quark star structure

The calculation of the structure of the quark star models for given values of the central density is giving by solving numerically the Tollman-Oppenheimer-Volkoff (TOV) equations (Tolman 1939; Oppenheimer & Volkoff 1939):

$$\frac{dP}{dr} = -G \frac{m(r)\varepsilon(P)}{(rc)^2} \left(1 + \frac{P}{\varepsilon}\right) \left(1 + \frac{4\pi r^3 P}{m(r)c^2}\right) \left(1 - 2G \frac{m(r)}{rc^2}\right)^{-1}, \quad (27)$$

and

$$\frac{dm(r)}{dr} = 4\pi r^2 \varepsilon. \quad (28)$$

The obtained results show that larger values of Δ_{CFL} and the current strange quark

Table 1: Set of the used model parameters. The density-dependent mass model parameters C and m_{s0} are in units of $MeV.fm^{-3}$ and MeV , respectively. The free characteristic gap parameter μ^* is in units of MeV .

μ^*	$C = 100, m_{s0} = 50$	$C = 90, m_{s0} = 80$	$C = 80, m_{s0} = 100$	$C = 70, m_{s0} = 150$
100	A1	B1	C1	D1
150	A2	B2	C2	D2
200	A3	B3	C3	D3
250	A4	B4	C4	D4

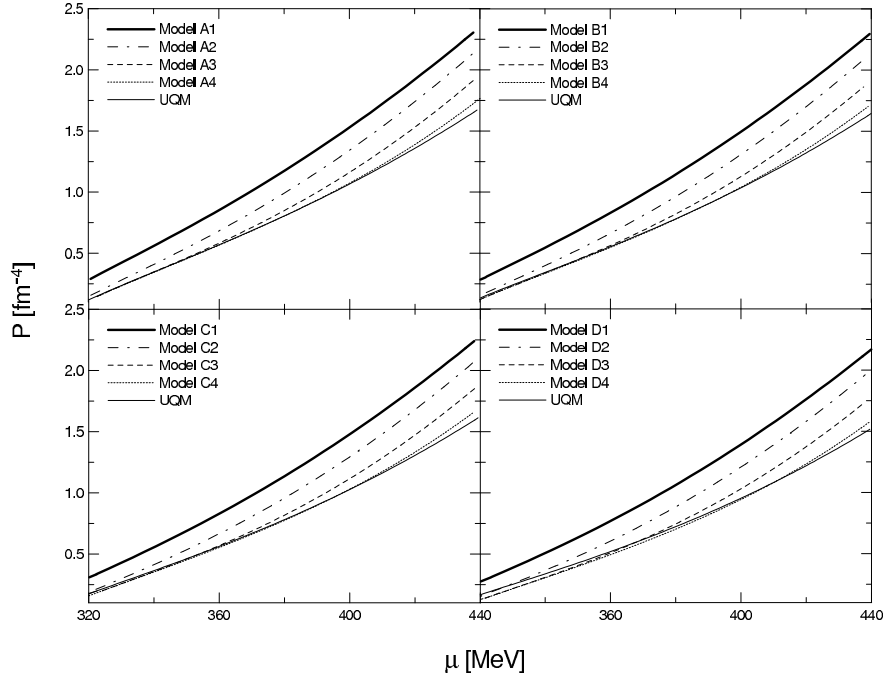


Fig. 3.— Pressure for different values of the model parameters given in Table 1, and for the unpaired quark matter phase as functions of the quark chemical potential.

mass tend to give more massive and larger quark stars. With an appropriate choice of the gap parameter μ^* , it is possible to obtain masses and radii compatible with the neutron stars calculated with equation of states widely used to nuclear and hadronic matter. Consequently, suitable selection of quark matter equation of state may lead to similar observational results obtained in different constitutive theoretical frameworks to the dense stellar matter composition.

In the panel showed in the Fig. 4 we compare the limits of mass and radius given in the Özel's works with those of quark stars calculated in this work, considering only the regime of strong coupling with $G_D = G_S$. Our results have been obtained for all sets of values of the parameters given in Table 1. The corresponding quark star models can reach a mass of $2.25 M_\odot$ and radius $11.4 km$, for $\mu^* = 250 MeV$, as showed in part-a of the panel, up to the maximum value $2.73 M_\odot$ with the radius $13.3 km$, for $\mu^* = 100 MeV$, as showed in part-d of the panel. For the sake of comparison, we show in the same panel the lower limits on the mass and radius of the neutron star EXO 0748-676, with the values of mass and radius given by $M = 2.10 \pm 0.28 M_\odot$ and $R = 13.8 \pm 1.8 km$. The one- and two- σ error bars of the results obtained by Özel are shown (dashed bars). Özel have found two pairs of values for the mass and radius of the neutron star in EXO 1745-248, which are centered around $M = 1.4 M_\odot$ and $R = 11 km$ or around $M = 1.7 M_\odot$ and $R = 9 km$. The one- and two- σ contours for its mass and radius are represented by the dark and soft grey regions, respectively. For the neutron star in 4U 1608-52 the obtained values are $M = 1.84 \pm 0.09 M_\odot$ and $R = 9.83 \pm 1.24 km$.

We can see that the obtained values of masses and radii for pure strange quark star models are in good agreement with those given by Özel in the references (Özel 2006) and (Güver et al 2010), and only in fair accordance with present data obtained for the compact star EXO 1745 – 248, which corresponds to the smallest radius of the set of compact

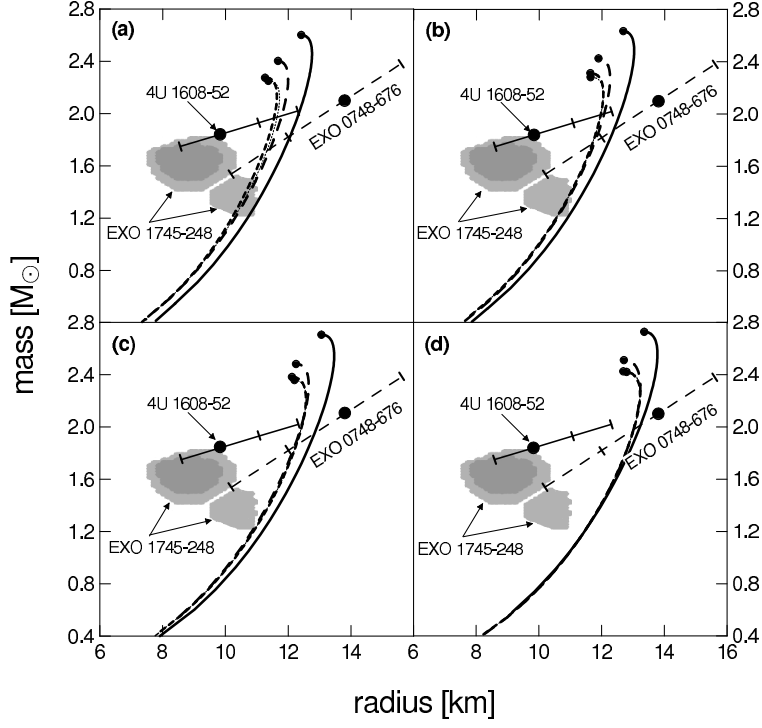


Fig. 4.— Mass-radius diagrams for the stable quark stars. The cases A1 to A4 given in Table 1 are shown in part-a; the cases B1 to B4, in part-b; the cases C1 to C4, in part-c; and the cases D1 to D4 in part-d. In all parts of the panel the solid lines stand for the models A1, B1, C1, and D1 ($\mu^* = 100 \text{ MeV}$); the long-dashed curves are for the models A2, B2, C2, and D2 ($\mu^* = 150 \text{ MeV}$); the short-dashed curves represent the models A3, B3, C3, and D3 ($\mu^* = 200 \text{ MeV}$); and the thin dotted curves represent the models A4, B4, C4, and D4 ($\mu^* = 250 \text{ MeV}$). It is also shown the lower limits on the mass and radius of the neutron star *EXO 0748 – 676*, given by $M = 2.10 \pm 0.28 M_\odot$ and $R = 13.8 \pm 1.8 \text{ km}$. The one- and two- σ error bars of the results obtained by Özel are also shown (dashed bars). Regarding the neutron star in *EXO 1745 – 248*, Özel have found two pairs of values for the mass and radius, which are centered around $M = 1.4 M_\odot$ and $R = 11 \text{ km}$ or around $M = 1.7 M_\odot$ and $R = 9 \text{ km}$. The one- and two- σ contour lines for its mass and radius are represented by the two gray regions. For the neutron star in *4U 1608 – 52* the obtained values are $M = 1.84 \pm 0.09 M_\odot$ and $R = 9.83 \pm 1.24 \text{ km}$. The one- and two- σ error bars of the new results obtained by Özel are shown (solid bars). For all error bars in the figure the one- σ are in both directions and the two- σ are only in one direction.

stars showed in the figure. From the result obtained for this class of object we thus can infer that such type of small compact stars, with small radii, are not natural candidates for pure quark stars, as it happens for the other ones, more massive and with larger radii. Nevertheless, small compact stars may be identified with hybrid stars composed of a quark matter core surrounded by a hadronic envelope. The present quark matter equation of state could still be helpful to describe the quark matter in the core of these hybrid structures.

5. Quark star with a nuclear crust

The strange quark matter in CFL phase is electrically neutral since the Cooper quark pairing minimizes the energy if the quarks have equal Fermi momenta. In this situation, the number of u , d and s quarks are equal and the bulk electric charge is zero without the need of electrons in the medium. However, even for strange quark matter in the CFL phase, when surface effects are taken into account, the number of massive quarks is reduced near the boundary of the star relative to the number of massless quarks at fixed Fermi momenta values. Consequently, there is a net quark charge at the very thin surface of the system. The thickness of the charged surface layer of the CFL quark star is $\sim 1\text{ fm}$, as it was discussed in references (Jaffe 1987; Madsen 2001; Usov 2004). The presence of such strong electric fields near the surface of the CFL strange star, make possible the existence of nuclear crusts spatially separated from the deconfined CFL quark core (Weber 2005).

Therefore, in order to investigate the change in the quark star structure with the inclusion of a nuclear matter crust, we have constructed an equation of state for the crust assuming that cold stellar matter in this crust is composed of a nuclear lattice immersed in an electron gas. To describe this crust matter we have used the equation of state given in (Baym et al 1971). Hence, we can find equilibrium configurations compatible with the solution of the TOV equations using this equations of state connected to the CFL matter

equation of state previously constructed.

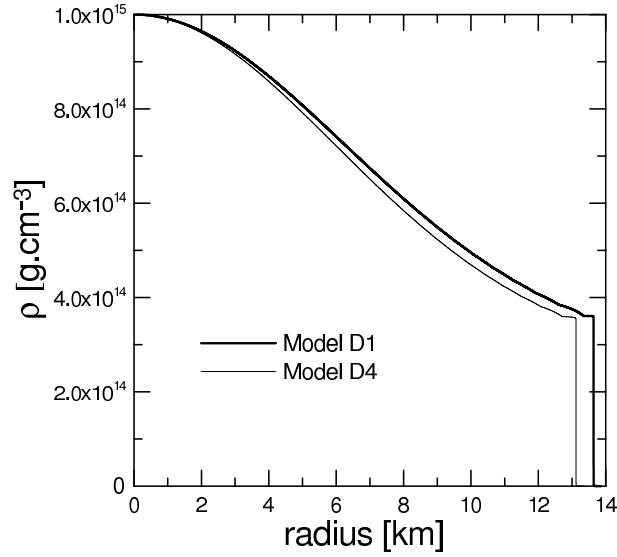


Fig. 5.— Energy density versus radius of quark stars with central density $\rho_c = 1.0 \times 10^{15} \text{ gcm}^{-3}$ for the models D1 and D4 given in Table 1.

In Fig. 5 we depict the energy density as a function of radius for two quark star models with the central density $1.0 \times 10^{15} \text{ gcm}^{-3}$, for the set of parameters D1 and D4 of Table 1. In the figure are depicted the density as a function of radius for two compact stars with dense and large cores. That one corresponding to the set of parameters D4 ($\mu^* = 100 \text{ MeV}$) is composed entirely of deconfined quarks in the *CFL* phase, and the other one, for the case A1 ($\mu^* = 250 \text{ MeV}$) is made of unpaired quarks. The obtained masses for these two compact stars are $2.69 M_\odot$, for the first model, and $2.37 M_\odot$, for the second one.

Figure 6 shows the detailed structure of the nuclear crusts enveloping the quark matter cores of the model compact stars shown in the previous figure. The thickness of these nuclear crusts are 196 m , for the model D1 ($\mu^* = 100 \text{ MeV}$), and 231 m for the model D4 ($\mu^* = 250 \text{ MeV}$).

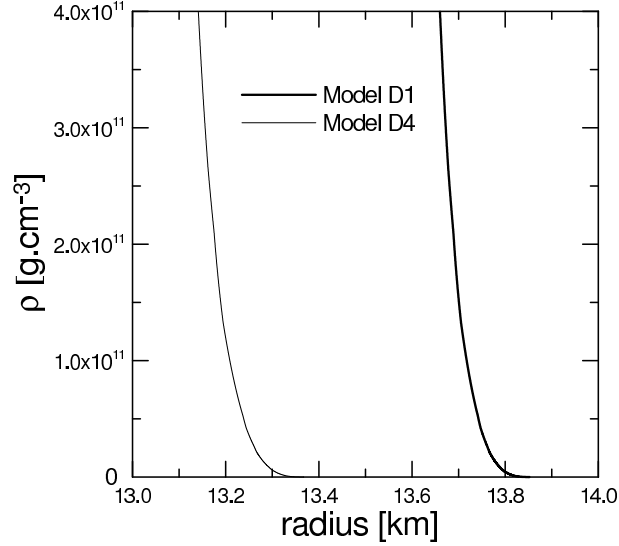


Fig. 6.— Details of the nuclear crusts of the quark stars displayed in the last figure.

In Fig. 7 are displayed the energy density as a function of radius for two quark stars with the central density $3.0 \times 10^{15} \text{ gcm}^{-3}$, again using the set of parameters of the models D1 and D4. For the model D1 the obtained quark star has a large core composed entirely of deconfined quarks in the *CFL* phase, and for the model D4 the large and dense core is composed of *CFL* quark phase enveloped by an unpaired quark shell. The obtained masses are $2.56 M_{\odot}$, for the the case D1, and $2.28 M_{\odot}$, for the case D4. The detailed structures of the nuclear crusts enveloping the quark stars shown in the previous figure are displayed in Fig. 8. The thickness of these nuclear crusts are $150 m$, for the first one, and $169 m$, for the second one.

The obtained results indicate that smaller values of μ^* correspond to more massive and less compact quark stars, almost entirely composed of quark matter. An interesting implication of the obtained results is that for increasing *CFL* gap energies one obtains smaller nuclear crusts. However, the *CFL* quark star will be naked only for a very unrealistic high value of the *CFL* gap energy.

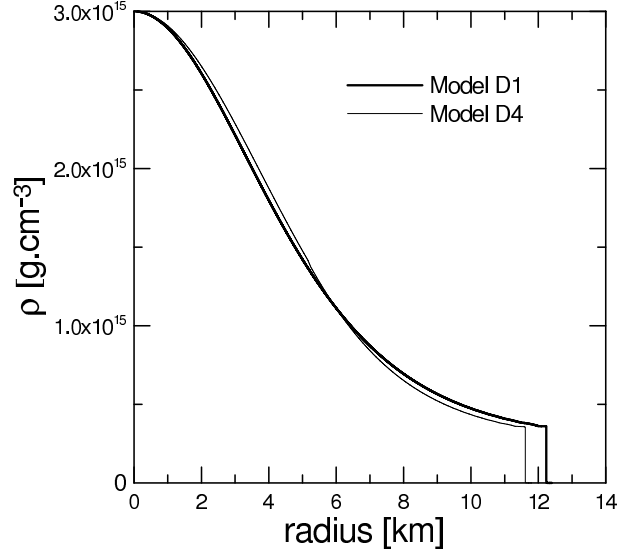


Fig. 7.— Energy density versus radius of quark stars with central density $\rho_c = 3.0 \times 10^{15} \text{ gcm}^{-3}$ for the models D1 and D4 given in Table 1.

Observe that the maximum density at the base of the nuclear crust which envelopes the quark star is determined by the threshold density for neutron drip ($\rho \sim 4.0 \times 10^{11} \text{ gcm}^{-3}$). On the other hand, the equal values of pressure at the surface of the quark matter core and the base of the nuclear crust is necessary to assure the hydrostatic equilibrium of the quark star as a whole.

6. Conclusions

In this work we have studied the properties of quark matter applying the density-dependent quark mass model in the calculation of the equation of state of the color superconducting quark matter. Within this framework, we have investigated the quark star structure for suitable values of the model parameter C , the current mass of the quarks, and the CFL gap energy, and so we have discussed the dependence of the observable

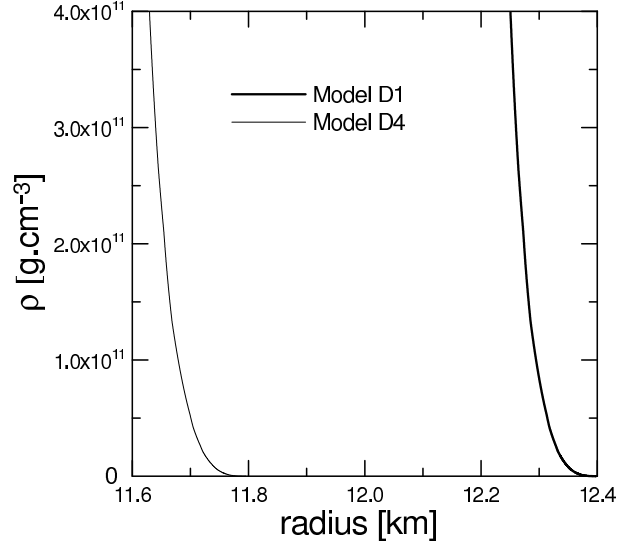


Fig. 8.— Details of the nuclear crusts of the quark stars displayed in the last figure.

properties of quark stars, such as maximum mass and radius, on the *CFL* gap energy.

In the present phenomenological analysis, we have used a color superconducting gap parametrization derived from microscopic approaches widely applied to describe color superconducting quark matter. The density-dependent quark mass model is also used in order to mimic the quark chiral symmetry behavior.

According to our results, the existence of the reported massive compact stars can be compatible with stable quark stars with a nuclear crust, or even bare quark stars.

The results presented here show that massive compact stars with mass $\gtrsim 2M_{\odot}$ up to maximal masses $2.73 M_{\odot}$ would be interpreted as compact stars composed entirely of deconfined quarks, in the color superconducting phase or even in the unpaired phase. Moreover, less massive and smaller compact stars would be identified with hybrid stars composed of a deconfined quark phase in the inner core enveloped by a hadronic phase, spatially separated due to the gravitational action. This configuration is allowed since

the burning of nuclear matter into quarks must be an exothermic process. This specific situation can occur for a range of densities, which are determined by the equations of state used to describe both phases, as shown in Refs. (Lugones 1994, 1995).

As a final remark, we call attention that the observational data obtained for compact objects which are possible candidates to be quark stars could be used to constrain the parameters of phenomenological models involved in the quark matter equation construction.

The authors are grateful to F. Weber for valuable discussions. The authors would like to thank the referee for the fruitful and clarifying discussions during the preparation and revision of the manuscript. H. Rodrigues and S. B. Duarte thank CNPq for financial support.

REFERENCES

- Alford M., Rajagopal K., & Wilczek F. 1998, Phys. Lett. B, 422, 247
- Alford M., Rajagopal K., & Wilczek F. 1999, Nucl. Phys. B, 537, 443
- Alford M., Berges J., & Rajagopal, K. 1999, Nucl. Phys. B, 558, 219
- Alford M. 2004, Prog. Theor., Phys. Suppl., 153, 1
- Alford M., Braby M., Paris M., & Reddy S. 2005, ApJ, 629, 969
- Alford M., Blaschke D., Drago A., Klähn T., Pagliara G., & Schaffner-Bielich J. 2007, Nature, 445, E7
- Alford M., Schmitt A., Rajagopal K., & Schäfer T. 2008, Rev. Mod. Phys., 80, 1455
- Barret D., Olive J. F., & Miller M. C. 2005, MNRAS, 361, 855
- Baym G., Pethick C., & Sutherland P. 1971, ApJ, 170, 299
- Benvenuto O. G., & Lugones G. 1995, Phys. Rev. D, 51, 1989
- Berger M. S., & Jaffe R. L. 1987, Phys. Rev. C, 35, 213. 1991, Phys. Rev. C, 44, 566 (E)
- Bodmer A. R. 1971, Phys. Rev. D, 4, 1601
- Braun-Muzinger P. & Wambach J. 2006, Re. Mod. Phys., 81, 1031
- Chakrabarty S., Saha S., & Sinha B. 1989, Phys. Lett. B, 229, 112
- Chakrabarty S. 1991, Phys. Rev. D, 43, 627
- Cottam J., Paerels F., & Mendez M. 2002, Nature, 420, 51
- Güver, T., Özel F., Cabrera-Lavers A., & Wroblewski, P. 2010, ApJ, 712, 964

- Itoh N. 1970, Prog. Theor. Phys., 44, 291
- Kurkela A., Romatschke P., & Vuorinen A. 2010, Phys. Rev. D, 81, 105021
- Lugones G., Benvenuto O. G., & Vucetich H. 1994, Phys. Rev. D, 50, 6100
- Lugones G., & Benvenuto O. G. 1995, Phys. Rev. D, 52, 1276
- Madsen J. 2001, Phys. Rev. Lett., 87, 172003
- Nice D. J., Splaver E. M., Stairs I. H., Loehmer O., Jessmer A., Kramer M., & Cordes J. M. 2005, ApJ, 634, 1242
- Oliveira J. C. T., Rodrigues H., & Duarte S. B. 2008, Phys. Rev. D, 78, 123008
- Oppenheimer J. R., & Volkoff G. M. 1939, Phys. Rev., 55, 374
- Orsaria M. G., Rodrigues H., & Duarte S. B. 2007, Int. J. Mod. Phys. D, 16, 291
- Özel, F. 2006, Nature, 441, 1115
- Özel F., Güver T., & Psaltis D. 2009, ApJ, 693, 1775
- Rajagopal K. & Wilczek F. 2001, Phys. Rev. Lett., 86, 16, 3492
- Rajagopal K. & Wilczek F. 2001, The Condensed Matter Physics of QCD, at the Frontier of Particle Physics/Handbook of QCD, ed. M. Shifman, World Scientific
- Rapp, R., Schäfer, T., Shuryak, E. V., & Velkovsky, M. 2000, Ann. Phys (N.Y.), 280, 35
- Rodrigues H., Duarte S. B., & Oliveira J. C. T. 2010, Nucl. Phys. B (Proc. Suppl.), 199, 333
- Rüster S. B., Werth V., Buballa M., Shovkovy I. A., & Rischke D. H. 2005, Phys. Rev. D, 72, 034004

Schmitt A. 2010, arXiv: 1001.3294v2 [astro-ph SR]

Schäfer & Wilczek F. 1999, Phys. Rev. D, 60, 074014

Tolman R. C. 1939, Phys. Rev., 55, 364

Trümper J. E., Burwitz V., Haberl F., & Zavlin V. E. 2004, Nucl. Phys. Proc. Suppl., 132, 560

Usov V. V. 2004, Phys. Rev. D, 70, 067301

Weber F. 2005, Prog. Part. Nucl. Phys., 54, 193

Witten E. 1984, Phys. Rev. D, 30, 272